An IoT-Based Controller Realization for PV System Monitoring and Control

Chapter · June 2020

DOI: 10.1007/978-3-030-44407-5_13

5 authors, including:

Jyoti Gupta
Thapar University
39 PUBLICATIONS **283** CITATIONS
SEE PROFILE

Manish kumar Singla
Chitkara University
50 PUBLICATIONS **596** CITATIONS
SEE PROFILE

Parag Nijhawan
Thapar University
84 PUBLICATIONS **772** CITATIONS
SEE PROFILE

Souvik Ganguli
Thapar University
822 PUBLICATIONS **11,542** CITATIONS
SEE PROFILE

Chapter 13
An IoT-Based Controller Realization for PV System Monitoring and Control

Jyoti Gupta, Manish Kumar Singla, Parag Nijhawan, Souvik Ganguli, and S. Suman Rajest

13.1 Introduction

In the recent era, the rapid increase in the consumption of electricity and issues regarding environmental concerns are the main reasons behind the development of renewable energy sources (RESs). The electricity generation from RES has been derived for its economic benefits and reliability [1]. Micro-grid includes distributed generation resources such as photovoltaic, wind, diesel generators, etc. The implementation of micro-grid in the distribution network was introduced in the early years of 2000 and encouraged by various agencies and utilities. Micro-grid has increased the operation of power electronics converter in the power system for efficient and effective power quality [2]. The micro-grid in a distribution system can be installed near the substation or at the end of the feeder. Micro-grid has an essential and useful feature, i.e., it can be operated in two different modes, islanded and grid-connected mode, to give essential support during the time of grid failure or maintenance of grid system by supplying constant power. Due to an increase in the interconnection of micro-grid in the distribution system, it raises some problems that include fluctuation in the voltage, steady-state over-voltage, increases in the system loss, and issues related to the voltage regulation devices and protection; therefore, appropriate allocation of micro-grid is desirable.

There are various types of micro-grids, namely, DC micro-grid, AC micro-grid, and hybrid micro-grid, which combines both AC and DC micro-grids [3]. Solar energy systems are dependent on two factors: temperature and irradiance. The max-

J. Gupta · M. K. Singla · P. Nijhawan · S. Ganguli (✉)
Thapar Institute of Engineering and Technology, Patiala, India
e-mail: jgupta_phd19@thapar.edu; souvik.ganguli@thapar.edu

S. S. Rajest
Vels Institute of Science, Technology & Advanced Studies, Chennai, India

A. Haldorai et al. (eds.), *Business Intelligence for Enterprise Internet of Things*,
EAI/Springer Innovations in Communication and Computing,
https://doi.org/10.1007/978-3-030-44407-5_13

imum power point (MPP) is the point where maximum power output is produced by PV array. The control scheme is developed using a neural network. A neural network (NN) is designed to provide a gate pulse signal to the inverter circuit to improve the performance of the system. The artificial neural network (ANN) is based on a machine learning approach and contains the number of artificial neurons to perform the specific task in the system [4]. To investigate its impact in different conditions, the inverter control scheme is used to improve the efficiency of the power transfer between the PV system and the grid. An IEEE 13-node test feeder system is considered as a grid system and is commonly used to test features of a standard distribution network of a power system, operating at 4.16 kV.

The main problem that arises in monitoring the output power of the photovoltaic system is the accuracy and time duration for the detection of the fault and the appropriate solution to it. The best approach for dealing with such kind of issues is the Internet of Things (IoT) [5, 6]. It is the new concept which has emerged recently and has gained a lot of attention in a few years. It can be generally explained as an information sharing environment where elements of the system are attached to a wireless and wired network. These days, this concept is not only applicable in the field of electronics but also in the area of home appliances, smart cars, industrial security, etc.

For the individuals and companies associated with solar panels, the IoT makes it possible to increase the MPPT reliability and performance of the system [7, 8]. For the controlling or monitoring of the system, the proposed method is discussed in the chapter.

13.2 Micro-grid Model Description

An IEEE 13-node test feeder system is considered as a grid system and is commonly used to test features of a standard distribution network of a power system, operating at 4.16 kV.

13.2.1 Photovoltaic Module

> The photovoltaic system operates on the principle of the photovoltaic effect, that is, when sunlight is radiated upon the semiconductor diode, there is a movement of electrons from P-type to N-type side of the semiconductor which produces the current in the system [10].

The photovoltaic module is simulated in MATLAB/Simulink using a photovoltaic array. To generate power of 341.65 kW, the SunPower SPR-445NX-WHT-D model is used, selected from the module block in the PV array block. Also, there are 8 series-connected modules and 96 parallel-connected modules per string. The module parameters and data are shown in Table 13.1. These values are calculated standard temperature and irradiance, i.e., 25°C and 1000 W/m^2 irradiance.

Table 13.1 Model parameters of PV array

Name of the parameters	Number/rating
Maximum power (watt)	444.86
Cell per module	128
Light generated current I_p(A)	6.2167
Diode saturation current I_D (A)	1.3552e-11
Shunt resistance R_{sh} (ohm)	508.2463
Series resistance R_{se} (ohm)	0.54861

13.2.2 DC-Link Capacitor and Inverter Circuit

A three-phase inverter circuit is connected across the DC link. DC-link capacitors are employed to stabilize the DC-link voltage of the grid-connected inverter. Due to temperature and irradiance variation to the total resistance within PV cells leading to non-linear output efficiency, capacitance is needed to allow electronic control methods to maintain maximum output power. The three-phase inverter converts the DC output voltage, i.e., 590V, from micro-grid into AC output, i.e., 240V.

13.2.3 RL Filter, Transformer, and Load

RL filter is connected at the three-phase inverter circuit output, to reduce the total harmonics distortion in the current. They prevent overcurrent condition in the system. A three-phase coupling transformer is between the micro-grid system and grid. Three-phase coupling transformer, star to the delta, is connected to step-up the voltage from 240V to 4160V at 50Hz frequency. It has a winding resistance of 0.01 per unit. The load is the distributed load of IEEE 13-node feeder systems.

13.2.4 Point of Common Coupling and Grid

Point of common coupling is described by using circuit breakers between PV system and grid system; it plays a vital role in the proposed method by isolating the PV system from grid system, i.e., in the islanded mode at the time of grid blackout or when grid is under maintenance and to supply power to particular load in case of deficit energy produced by micro-grid. Grid is a standard IEEE 13-node test feeder system, as displayed in Fig. 13.1.

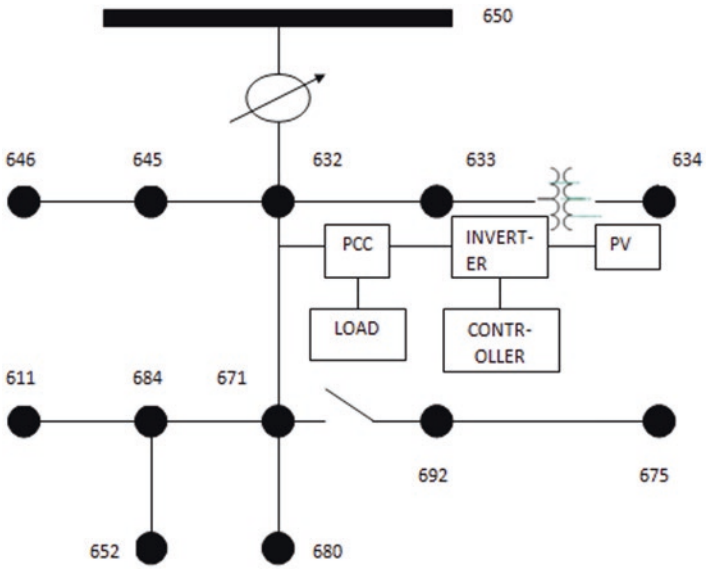

Fig. 13.1 Block representation of micro-grid-connected grid system [9]

13.3 Proposed Control Features

Micro-grid is mainly operated in two modes, i.e., islanded and grid-connected. The proper controlling action of micro-grid is an essential condition for steady and efficient operation in every mode. The controller performs the following functions:

- Control of the power flow between the grid system and micro-grid.
- Proper synchronization of micro-grid with the grid system.
- Proper regulation of load sharing between the grid system and micro-grid.
- Regulation of the frequency and voltage for both operating modes, namely, grid-connected and islanded mode.
- Re-optimization of the operation cost of the micro-grid.
- While operating during the switching modes, proper handling of transients and restoration of the desired condition are necessary.

13.3.1 MPPT Controller

Maximum power point tracking (MPPT) is the algorithm which extracts the maximum power from the photovoltaic system generated by photovoltaic cell or module at the specific environmental condition. The specific voltage at which solar device generates maximum power output is called maximum power point. There are various types of techniques used for maximum power point tracking, out of which perturb and observe algorithm is used in this work for determining the maximum power point of

the photovoltaic module. This technique uses only one sensor to detect the maximum power point that is a voltage sensor. It also reduces the cost and complexity of the system. This technique is quite easy as it has the least time complexity [11, 12].

13.3.2 Inverter Controllers

13.3.2.1 PI Controller

The inverter controller operates on the double closed-loop current algorithm. There are two loops, outer and inner loop. The voltage control loop is referred to as the outer loop, and its primary duty is to maintain the DC voltage of PV array. A current control loop is referred to as the inner loop, and its primary duty is to keep the active and reactive current signal of the grid (I_d and I_q). For stabilizing the power factor at unity for efficient grid interconnection, the voltage control loop provides the output of I_d, which is the reference of current, while keeping I_q value regulated to minimum, i.e., zero, using a PI controller to minimize error. The inner control loop provides the voltage output V_d and V_q. The tracking error can be reduced, and tracking speed can be increased by regulating the PI controller in the inner current control loop. Forward-feed compensation output is included in the loop to decrease the disadvantages to the perturbation of the voltage of grid.

The phase-locked loop (PLL) algorithm is applied to regulate the values of the active power and reactive power injected into the IEEE 13-node feeder systems. The advantage of a phase-locked loop is that it helps in locking and synchronizing the frequency and phase angle output of the voltage with reference to the current of the grid using transformations. The output of the current control loop and voltage control loop is feed to the converter block whose function is to sense the vector values of current and voltage, respectively and convert theses values into the d-q reference frame as DC quantities. The output of the converter block is then feed to over modulation in order to increase the linear region of a three-phase PWM modulator by approximately 15%. The output is transferred to PWM three-level pulse generators to produce the input pulse to the inverter.

13.3.2.2 Artificial Neural Network Controller

An artificial neural network is a massively parallel distributed processor consisting of simple processing units, which has an inherent property to store knowledge of experiments and make it available for use. In two respects it resembles the brain as follows:

- The strengths of the interneuron connection, known as synaptic weights, are used to store the knowledge gained.
- The network acquires knowledge from its environment through a learning process.
- Mathematically, neuron modeling can be represented by the following Eqs. 13.1, 13.2 and 13.3:

$$u_k = \sum_{j=1}^{M} w_{kj} x_j \tag{13.1}$$

$$y_k = \varphi\left(u_k + b_k\right) \tag{13.2}$$

$$v_k = u_k + b_k \tag{13.3}$$

where x_j denotes the inputs, w_{kj} represents the synaptic weights of the neuron k, u_k is the combined output due to the inputs, b_k is the bias, $\varphi(.)$ is the activation function, and y_k is the output signal of the neuron. The use of bias has the effect of applying an affine transformation to the linear combiner output u_k in the modeling process.

Levenberg-Marquardt algorithm is used to train the neural network, which is the second-order optimization of the backpropagation algorithm. This algorithm typically requires less time and is robotic. This algorithm typically requires less time and is robust, which are the advantages of this algorithm over the Gauss-Newton algorithm and gradient descent method. The flow chart explaining the process of a neural network is shown in Fig. 13.2.

13.3.2.3 Monitoring System

Mainly two main MPPT designing variables, perturbation period (Tp) and perturbation magnitude (x), can be used as metrics. For the higher-resolution system, a smaller metric has greater acceptability [13–15]. The primary constraint of the mentioned system is the speed at which it receives and regulates the desired information. The constraints of the MPPT variable Tp are described in Eq. 13.4.

$$Tp >= \frac{-\ln\left(\frac{\in}{2}\right)}{\delta.\omega_n} \tag{13.4}$$

where w_n is the natural frequency of the defined inverter system, δ is the damping factor of the system, $\in$ is the controlling variable of the system, and mainly, 0.1 is the assigned value. The constraints of variable (x) are described in Eq. 13.5.

$$x > \frac{1}{\mu}.\sqrt{A.Kph.|G|.Tp} \tag{13.5}$$

Here, μ is the static gain of the inverter, *Kph* is the PV material constant related to the spectral-averaged responsiveness, G is the average of the irradiance slope, and A is the combination of dependent variable irradiance [16, 17]. Figure 13.3 represents the block diagram of the IoT-based MPPT system of the modules.

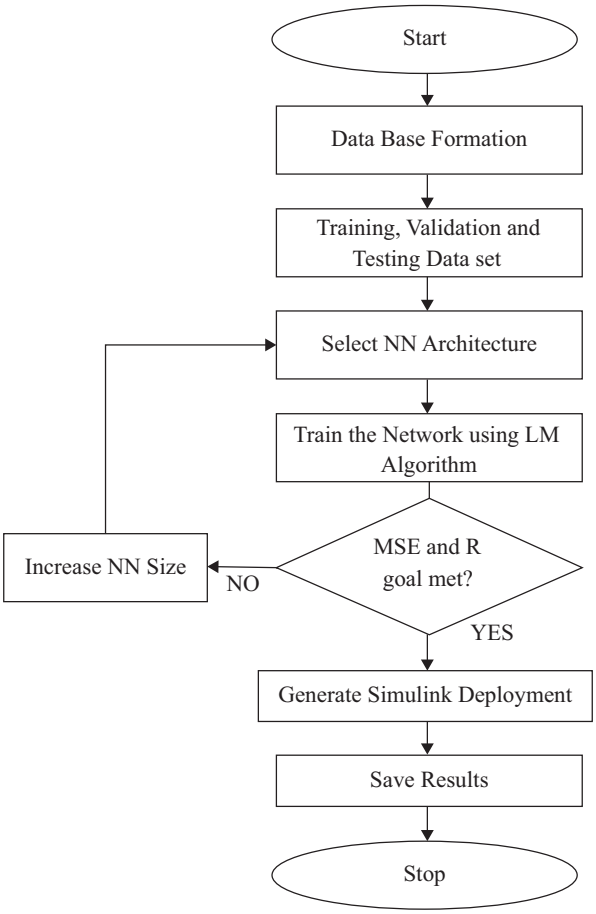

Fig. 13.2 Flow diagram of ANN

13.4 Results and Discussions

The system is simulated in Simulink for 0.75 s with the following parameters: frequency of 50Hz at standard irradiance and temperature and 590V. The allocation of PV system between the load bus 632 and 631 in the IEEE 13-node feeder system is decided by the calculation of the central position in the grid using line segment data.

The inverter circuit is controlled by using a standard PI controller and neural network. The power quality results using both the controllers are compared. The power quality results include power output, voltage deviation, total harmonic distortion, and phase angle deviation, which are observed as shown in Figs. 13.4 (a), 13.4(b), 13.5(a), 13.5(b), and 13.6, respectively.

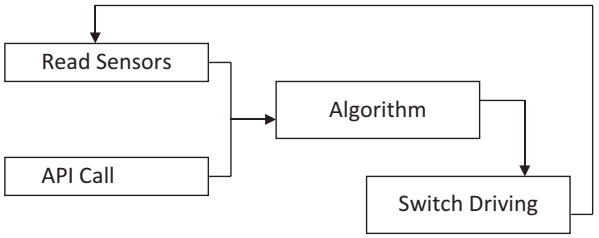

Fig. 13.3 IoT-based MPPT system [17]

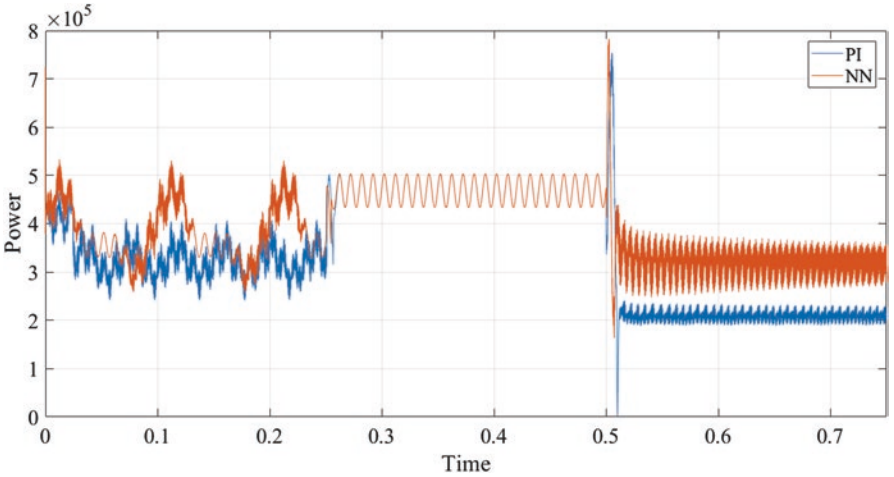

(a) Power output across the load

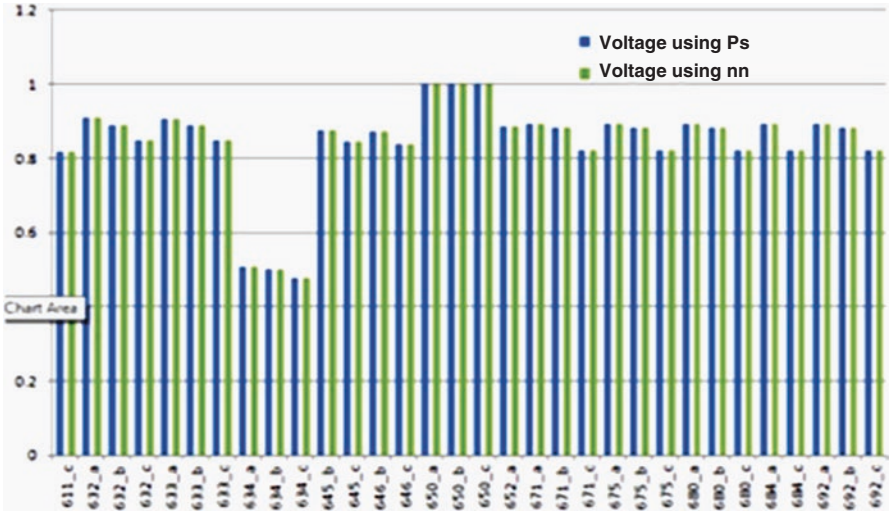

(b) Voltage deviation at different buses

Fig. 13.4 (**a**) Power output across the load. (**b**) Voltage deviation at different buses

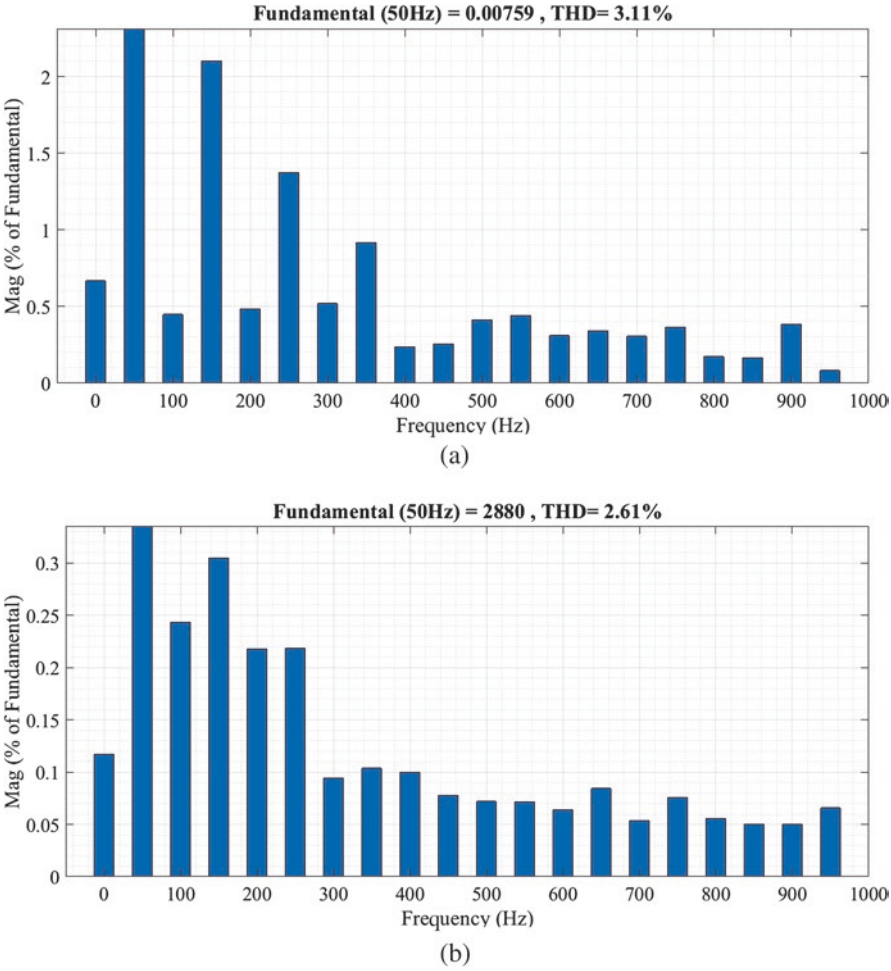

Fig. 13.5 (**a**) FFT using PI and (**b**) FFT using NN

The output graphs of the power quality are divided into three half-sections:

1. The first part is from 0 s to 0.25 s; at this time, system load is met by both PV system and grid, i.e., the system is operated at grid-connected PV mode.
2. The second part is from 0.25 s to 0.5 s; at this time, system load is met only by grid, i.e., PV output is not sufficient to meet the required load.
3. The third part is from 0.5 s to 0.75 s; at this time, system load is achieved only by PV system, i.e., PV output is sufficient to satisfy load, and the system is operated at islanded mode.

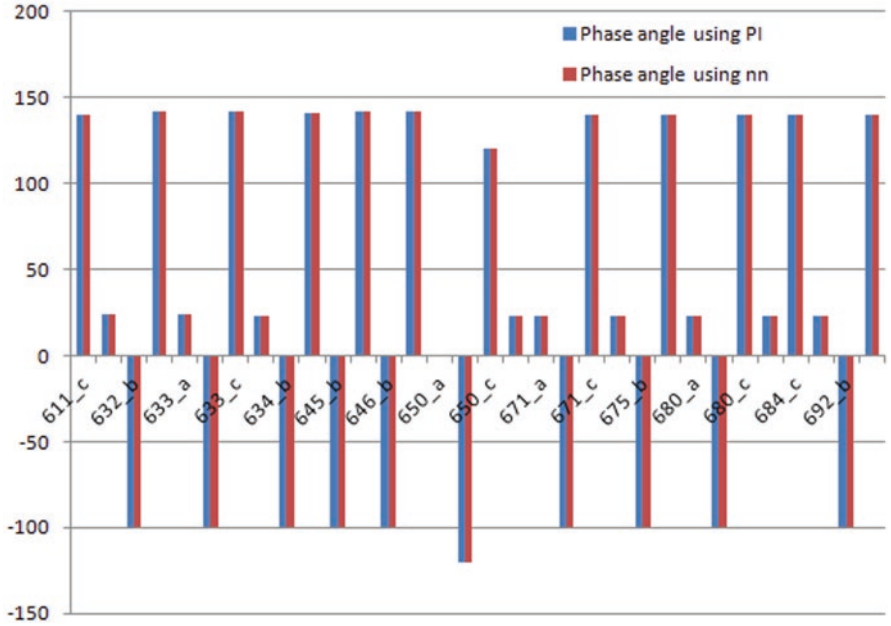

Fig. 13.6 Phase angle at different buses

13.5 Summary

It is presented that the interconnection of a photovoltaic system as a micro-grid improves the reliability of electric supply and power quality by regulating the IoT-based inverter controller systems. The IoT-based ANN inverter control scheme for the efficient and reliable power transfer between the grid system and micro-grid to satisfy the desired load is being demonstrated in this work. The IoT-based ANN-based controller response has also been compared with IoT-based PI controller, which justifies its technical feasibility.

References

1. Sadeghian, Hamidreza, Mir HadiAthari, & Zhifang Wang. (2017). Optimized solar photovoltaic generation in a real local distribution network. In *2017 IEEE Power & Energy Society Innovative Smart Grid Technologies Conference (ISGT)* (pp. 1–5). IEEE.
2. Lasseter, R. H. (2002). Micro-grids. In *2002 IEEE Power engineering society winter meeting. Conference Proceedings (Cat. No.02CH37309) 1* (pp. 305–308). IEEE.
3. Pham, D. H., Hunter, G., LiLi, & Zhu, J.. (2015). Advanced microgrid power control through grid-connected inverters. In *2015 IEEE PES Asia-Pacific Power and Energy Engineering Conference (APPEEC)* (pp. 1–6). IEEE.

4. Singh, K., Swathi, P., &Ugender Reddy, M.. (2014). Performance analysis of PV inverter in microgrid connected with PV system employing ANN control. In *2014 International Conference on Green Computing Communication and Electrical Engineering (ICGCCEE)* (pp. 1–6). IEEE.
5. Chen, X., Sun, L., Zhu, H., Zhen, Y., & Chen, H.. (2012). Application of internet of things in power-line monitoring. In *2012 International conference on cyber-enabled distributed computing and knowledge discovery* (pp. 423–426). IEEE.
6. Kang, B., Park, S., Lee, T., & Park, S.. (2015). IoT-based monitoring system using tri-level context making model for smart home services.In *2015 IEEE International Conference on Consumer Electronics (ICCE)* (pp. 198–199). IEEE.
7. Woyte, A., Richter, M., Moser, D., Mau, S., Reich, N., & Jahn, U.. (2013). Monitoring of photovoltaic systems: good practices and systematic analysis. In *Proceedings of the 28th European photovoltaic solar energy conference* (pp. 3686–3694).
8. Belghith, O. B., & Sbita, L.. (2014). Remote GSM module monitoring and photovoltaic system control.In *2014 First International Conference on Green Energy ICGE 2014* (pp. 188–192). IEEE.
9. Kersting, W. H.(2009). Distribution feeder voltage regulation control. In *2009 IEEE rural electric power conference* (pp. C1–C1). IEEE.
10. Villalva, M. G., Gazoli, J. R., & Filho, E. R. (2009). Comprehensive approach to modeling and simulation of photovoltaic arrays. *IEEE Transactions on power electronics, 24*(5), 1198–1208.
11. Chin, C. S., Tan, M. K., Neelakantan, P., Chua, B. L., & Teo, K. T. K. (2011). Optimization of partially shaded PV array using fuzzy MPPT. In *2011 IEEE colloquium on humanities, science and engineering* (pp. 481–486). Penang: IEEE.
12. Esram, T., & Chapman, P. L. (2007). Comparison of photovoltaic array maximum power point tracking techniques. *IEEE Transactions on Energy Conversion, 22*(2), 439–449.
13. De Brito, M. A. G., Galotto, L., Sampaio, L. P., de Guilherme, A. e. M., & Canesin, C. A. (2012). Evaluation of the main MPPT techniques for photovoltaic applications. *IEEE Transactions on Industrial Electronics, 60*(3), 1156–1167.
14. Esram, T., & Chapman, P. L. (2007). Comparison of photovoltaic array maximum power point tracking techniques. *IEEE Transactions on Energy Conversion, 22*(2), 439–449.
15. Beevi, S.Shanifa, J. M., & Vincent, G.. (2016). A high performance instantaneous resistance maximum power point tracking algorithm. In *20167th India International Conference on Power Electronics (IICPE)* (pp. 1–5). IEEE.
16. Ma, J., Man, K. L., Ting, T. O., Zhang, N., Guan, S. U., & Wong, P. W. H. (2014). Estimation and revision: A framework for maximum power point tracking on partially shaded photovoltaic arrays. In *2014 International symposium on computer, consumer and control* (pp. 162–165). Taichung: IEEE.
17. Bardwell, M., Wong, J., Zhang, S., & Musilek, P. (2018). Design considerations for IoT-based PV charge controllers. In *2018 IEEE world congress on services (SERVICES)* (pp. 59–60). San Francisco: IEEE.